

Permeabilities of teleost and elasmobranch gill apical membranes: evidence that lipid bilayers alone do not account for barrier function

Warren G. Hill,^{1,2*} John C. Mathai,^{1,2*} Rebekah H. Gensure,^{1,2} Joshua D. Zeidel,¹ Gerard Apodaca,¹ James P. Saenz,² Evamaria Kinne-Saffran,^{2,3†} Rolf Kinne,^{2,3} and Mark L. Zeidel^{1,2}

¹Laboratory of Epithelial Cell Biology, Renal-Electrolyte Division, Department of Medicine, University of Pittsburgh School of Medicine, Pittsburgh, Pennsylvania 15261; ²Mount Desert Island Biological Laboratory, Salisbury Cove, Maine 06472; and ³MPI für Molekulare Physiologie, 44227 Dortmund, Germany

Submitted 13 January 2004; accepted in final form 25 February 2004

Hill, Warren G., John C. Mathai, Rebekah H. Gensure, Joshua D. Zeidel, Gerard Apodaca, James P. Saenz, Evamaria Kinne-Saffran, Rolf Kinne, and Mark L. Zeidel. Permeabilities of teleost and elasmobranch gill apical membranes: evidence that lipid bilayers alone do not account for barrier function. *Am J Physiol Cell Physiol* 287: C235–C242, 2004. First published March 3, 2004; 10.1152/ajpcell.00017.2004.—Teleosts and elasmobranchs faced with considerable osmotic challenges living in sea water, use compensatory mechanisms to survive the loss of water (teleosts) and urea (elasmobranchs) across epithelial surfaces. We hypothesized that the gill, with a high surface area for gas exchange must have an apical membrane of exceptionally low permeability to prevent equilibration between seawater and plasma. We isolated apical membrane vesicles from the gills of *Pleuronectes americanus* (winter flounder) and *Squalus acanthias* (dogfish shark) and demonstrated approximately sixfold enrichment of the apical marker, ADPase compared to homogenate. We also isolated basolateral membranes from shark gill (enriched 2.3-fold for Na-K-ATPase) and using stopped-flow fluorometry measured membrane permeabilities to water, urea, and NH₃. Apical membrane water permeabilities were similar between species and quite low ($7.4 \pm 0.7 \times 10^{-4}$ and $6.6 \pm 0.8 \times 10^{-4}$ cm/s for shark and flounder, respectively), whereas shark basolateral membranes showed twofold higher water permeability ($14 \pm 2 \times 10^{-4}$ cm/s). Permeabilities to urea and NH₃ were also low in apical membranes. Because of the much lower apical to basolateral surface area we conclude that the apical membrane represents an effective barrier. However, the values we obtained were not low enough to account for low water loss (teleosts) and urea loss (elasmobranchs) measured *in vivo* by others. We conclude that there are other mechanisms which permit gill epithelia to serve as effective barriers. This conclusion has implications for the function of other barrier epithelia, such as the gastric mucosa, mammalian bladder, and renal thick ascending limb.

water; urea; epithelia; osmoregulation

IN PRIOR STUDIES, we and others have developed the concept of barrier apical membranes, which permit epithelia to maintain large osmotic and concentration gradients between the compartments they separate (5, 13, 17, 19, 22, 26, 27). These studies have established that water permeabilities of 10^{-4} cm/s and urea permeabilities of 10^{-6} – 10^{-7} cm/s are representative of the properties of isolated barrier apical membranes from epithelia, and further studies (15) have established the characteristics of lipid membrane structure necessary for a bilayer to

achieve these low permeability values and to function as an equally effective barrier.

Teleosts and elasmobranchs deal with the severe osmotic challenge of life in seawater (1,000 mosmol/kgH₂O) in different ways. Teleosts maintain a tissue osmolality of ~ 340 mosmol/kgH₂O by continuous drinking and gut absorption of seawater coupled with excretion of excess salt via the gills and operculum (16). By contrast, elasmobranchs maintain tissue osmolalities $\sim 1,000$ mosmol/kgH₂O by keeping high tissue concentrations of urea, which therefore balance the osmolality of the seawater (2, 28).

The gills enhance gas exchange by presenting a large surface area over which blood and seawater come into close contact. While effecting gas exchange, the gills must maintain a tight barrier to the efflux of water down its osmotic gradient in teleosts, and urea down its concentration gradient in elasmobranchs. Moreover, the gills are known to play an active role in ammonium/ammonia excretion (31). Prior measurements in intact animals and in freshly excised and perfused gill preparations have shown exceptionally low permeabilities to water and urea (2, 9, 21, 23), although some studies have noted that elasmobranchs appear to have higher water permeabilities than teleosts (4, 24). If the major barrier to water and urea flux resides in the cell membrane, particularly the apical cell membrane, then isolated apical membrane vesicles would be expected to exhibit exceptionally low permeabilities. Analysis of the lipid structure of these membranes would yield important insights into how such low permeability membranes could be formed (15).

To determine whether the apical membrane functions as the major barrier to flux in gill epithelia, we prepared apical membrane vesicles from the gill of a teleost, the winter flounder (*Pleuronectes americanus*), and of an elasmobranch, the dogfish (*Squalus acanthias*), and measured their permeabilities to water, urea, ammonia, and protons. To identify whether the apical or basolateral membrane serves as the barrier for each of these substances, we used a recently described method to purify basolateral membranes from dogfish gill epithelia as well (9). The results reveal that teleosts and elasmobranch gills share relatively low permeabilities to water and urea. However, these values are still too high to account for the barrier properties of the gill. Ammonia and proton permeabilities were relatively high. These results suggest that the gill has developed barrier mechanisms in addition to the apical membrane

* W. G. Hill and J. C. Mathai contributed equally to this study.

† Deceased December 6, 2002.

Address for reprint requests and other correspondence: M. L. Zeidel, Laboratory of Epithelial Cell Biology, Dept. of Medicine, Univ. of Pittsburgh School of Medicine, Rm. 1218, Scaife Hall, 3550 Terrace St., Pittsburgh, PA 15261 (E-mail: zeidel@msx.dept-med.pitt.edu).

The costs of publication of this article were defrayed in part by the payment of page charges. The article must therefore be hereby marked "advertisement" in accordance with 18 U.S.C. Section 1734 solely to indicate this fact.



itself that help reduce water and urea leakage across the epithelium. Such additional barrier mechanisms need to be defined if we are to understand the mechanism of barrier function in other barrier epithelia.

EXPERIMENTAL PROCEDURES

Apical membrane preparations. All experiments were approved by and complied with the protocols of the MDI Biological Laboratory Institutional Animal Care and Use Committee. Flounders were killed by decapitation and sharks by pithing. The heads were put on ice and the gill arches excised. Gill filaments radiating from the branchial arches of flounder were cut off, whereas intact excised shark gills were scraped with a glass slide and the epithelia recovered. An apical membrane fraction was prepared according to the method of Booth and Kenny (1). Tissues were placed in 35 ml of gill homogenization (GH) buffer composed of (in mM) 10 mannitol, 250 sucrose, 2 Tris·HCl, 2 5- (and 6-)carboxyfluorescein (pH 7.1) with one tablet of protease inhibitor cocktail (Complete Mini, Roche, Mannheim, Germany) and homogenized at 4°C for 30 s at full speed in a Waring blender. After a 60-s incubation on ice, homogenization for 30 s at full speed was repeated and the homogenate was filtered through gauze. The volume was brought up to 35 ml with GH buffer. A 1-ml sample was taken and stored at 4°C for determination of enzyme activities and protein content. CaCl₂ was added to a final concentration of 30 mM, and after 15 min on ice the suspension was centrifuged for 12 min at 1,500 g. The supernatant was collected and centrifuged for 20 min at 15,000 g, and then the pellet was resuspended in 25 ml of GH buffer without carboxyfluorescein and recentrifuged for 20 min at 15,000 g. This pellet wash was repeated twice more because it was necessary to remove extravascular carboxyfluorescein. The final pellet was suspended in 400 μ l of GH buffer by repeated passage through a 26-gauge needle. An aliquot (100 μ l) was removed for enzyme assays and stored at 4°C.

Basolateral membrane preparations. The method used was that of Fines et al. (9) with minor modifications. Briefly, scraped epithelial cells from two dogfish sharks (~1 kg each) were combined and diluted into 30 ml of hypotonic homogenizing solution composed of (in mM) 25 NaCl, 1 dithiothreitol, 0.5 EDTA, 1 HEPES, and 1 Tris·HCl, pH 8.0, to which one tablet of protease inhibitor cocktail was added. The scrapings were homogenized with 30 strokes each in a Dounce homogenizer with a loose-fitting and then a tight-fitting pestle. The homogenate was diluted to 100 ml in hypotonic homogenizing solution, and the whole homogenate was sampled for marker enzymes. The homogenate was centrifuged at 500 g for 15 min to remove nuclei and cell debris. The supernatants were pelleted at 50,000 g for 1 h, and the lighter portion of the pellet was washed off of the denser, dark mitochondria with 15-ml sucrose buffer composed of (in mM) 250 sucrose, 5 MgCl₂, 5 HEPES, and 5 Tris·HCl, pH 7.4, containing 5 carboxyfluorescein. The suspension was homogenized with 100 strokes using the tight-fitting pestle in the Dounce homogenizer. The second homogenate was centrifuged at 1,000 g for 10 min and then at 10,000 g for 10 min. The supernatant was then pelleted at 30,000 g for 45 min. This pellet was washed two to three times with sucrose buffer to remove extravascular carboxyfluorescein. This final pellet was brought up in 1–1.5 ml of sucrose buffer and used for permeability measurements, assays of marker enzymes, and measurements of vesicular size.

Marker enzyme assays. The membrane fractions were assayed for the marker enzymes ADPase (apical plasma membrane), Na-K-ATPase (basolateral plasma membrane), and succinate dehydrogenase (mitochondria). ADPase activity was determined at 25°C in an assay medium containing (in mM) 20 HEPES (pH 7.4), 5 MgCl₂, and 5 ADP. The assay medium for the determination of Na-K-ATPase activity contained 20 HEPES (pH 7.4), 100 NaCl, 20 KCl, 6 MgCl₂, and 3 ATP, in the absence or presence of 2 mM ouabain. After 30 min of incubation, ice-cold 10% trichloroacetic acid was added to the

samples to stop the reaction. The samples were then centrifuged, and the amount of liberated inorganic phosphate was determined in the supernatant according to Fiske and Subbarow (10).

Succinate dehydrogenase, a mitochondrial marker, was measured by adding membrane fractions (25 and 50 μ l) to 300 μ l of succinate solution (in mM: 10 sodium succinic acid and 50 Na₂HPO₄, to which 50 KH₂PO₄ is added until pH 7.4 is reached). Blanks containing membranes but with no substrate were also set up for each sample tested. Samples and blanks were incubated for 10 min at 37°C, and then 1 ml of top solution [10% (wt/vol) trichloroacetic acid, 50% (vol/vol) ethyl acetate, and 50% (vol/vol) ethanol] was added to blanks and 100 μ l of INT solution [2.5 mg/ml *p*-iodonitrotetrazolium violet in phosphate buffer (as per succinate solution)] was added to all tubes. Samples were incubated at 37°C for 20 min, and stop solution was then added to the nonblank samples. Absorbances were measured at 490 nm, and concentrations were calculated using a molar extinction coefficient of 19,300 cm⁻¹M⁻¹ for reduced INT.

Measurement of solute permeabilities. Permeabilities to water, urea, ammonia, and protons were measured at 15°C (unless otherwise stated) with the use of a stopped-flow fluorometer (model SX.17 MV, Applied Photophysics, Leatherhead, UK) with a measurement dead time of <1 ms, as previously described (5, 17, 27). To determine osmotic water permeability (P_f), vesicles containing 2 mM carboxyfluorescein were rapidly mixed with an equal volume of GH buffer (apical membranes) or sucrose buffer (basolateral membranes) that had three times the osmolality due to sucrose addition. Buffer osmolalities were determined on a freezing-point depression osmometer (model Osmette A, Precision Systems, Natick, MA). The rate of water efflux from vesicles was measured as a function of vesicle shrinkage and carboxyfluorescein self quenching. Typically, 8–10 quench curves were averaged and fit with a single exponential curve. To ensure that the only signal recorded was from intravesicular fluorescence, quenching antibody (Molecular Probes; Eugene, OR) was added before the experiment. From parameters which included the initial rate of quenching, vesicle diameter and applied osmotic gradient, P_f was calculated with the use of MathCad software (MathSoft; Cambridge, MA). Urea permeabilities were assayed by incubating membrane vesicles in GH or sucrose buffers containing 1 M urea for 30 min on ice. Rapid mixing of urea-loaded vesicles with GH or sucrose buffer containing 0.82 M sucrose (isoosmotic with respect to urea-containing buffer) permitted measurement of urea permeability rates. Urea efflux in response to the chemical gradient was followed by water efflux with subsequent vesicle shrinkage. Proton permeabilities were measured by stopped-flow fluorometry as described (5, 17, 27). This assay utilized pH-dependent quenching of carboxyfluorescein on exposure of liposomes to isoosmotic buffer at a reduced pH. The pH gradient was typically 0.4–0.6 pH units, which has been shown not to induce the formation of limiting potentials (8). Ammonia permeability was measured by the rapid mixing of vesicles with buffer containing 20 mM NH₄Cl and pH adjusted to 6.8. Before the experiment, vesicles were preequilibrated in GH or sucrose buffer, pH 6.8. At this lower pH, the NH₃:NH₄⁺ ratio is higher, increasing the gradient for NH₃, which may be calculated from the Henderson-Hasselbalch equation.

Determination of activation energy. Water permeabilities were measured at five different temperatures between 4 and 18°C. Activation energy (E_a) was calculated from the slope of the natural log of the rate plotted against 1/T, multiplied by the gas constant, R .

Determination of vesicle size. Vesicle size distribution was determined by quasi-elastic light scattering with the use of a particle sizer (model LSR, DynaPro, Charlottesville, VA) and DYNAMICS data collection and analysis software. Flounder gill apical membrane vesicles, shark gill apical membranes, and shark gill basolateral membranes were 308 \pm 6, 596 \pm 19, and 585 \pm 126 nm (means \pm SE, n = 4) in diameter, respectively. For all three preparations there were normal distributions, with a single peak exhibiting polydispersities (a measure of the distribution width) between 34 and 59%.

RESULTS

Purification of apical membrane vesicles from flounder and shark. Table 1 shows the enrichment of flounder and dogfish gill apical membranes using ADPase as an apical membrane marker and Na-K-ATPase as a basolateral membrane marker. ADPase was enriched 6.2- and 6.7-fold in the flounder and dogfish apical membrane preparations, respectively, whereas Na-K-ATPase was neither enriched nor deenriched. To ensure that ADPase represents an apical membrane marker, we biotinylated the apical surfaces of the gills in the flounder and measured purification of the biotin resulting from our preparative approach. The biotin was enriched 5.7-fold, in good agreement with the 6.5-fold enrichment of the ADPase (29). Electron micrographs of the flounder gill apical membrane preparation revealed a high proportion of membrane vesicles decorated by a prominent glycocalyx, which is characteristic of the apical epithelial surface (18, 25) (data not shown).

Vesicles demonstrate osmotic sensitivity. To ascertain that the membrane vesicles we had isolated would shrink or swell in a linear manner and that the entrapped fluorophore would report such volume changes in response to an osmotic challenge, we monitored the entrapped carboxyfluorescein (CF) fluorescence after addition of CF-quenching antibody. Because CF at the concentration we used increases or decreases fluorescence linearly with its concentration, it can be used to ascertain whether the vesicles are behaving as perfect osmometers. Shark gill apical membrane vesicles in GH buffer were placed in a cuvette with CF-quenching antibody and then exposed to incremental increases in osmotic gradient achieved by the addition of 2 M sucrose (Fig. 1A) or to hypotonic challenge through the addition of distilled water (Fig. 1B). CF fluorescence self quenches in response to vesicle shrinkage and dequenches if volume increases. As shown, gill vesicles exhibited linear swelling and shrinking responses to changes in osmotic conditions. Flounder gill vesicles exhibited the same behavior (data not shown).

Permeability properties of teleost and elasmobranch gill apical membranes. Figure 2 shows representative tracings of water (A and B) and urea (C and D) fluxes across gill epithelial apical membranes from flounder (A and C) and dogfish (B and D). Vesicles show single exponential decay kinetics (fitted curves) indicative of relatively homogenous populations. At 15°C, water permeability averaged $6.6 \pm 1.8 \times 10^{-4}$ cm/s (means \pm SE; $n = 4$) for flounder and $7.4 \pm 0.7 \times 10^{-4}$ cm/s ($n = 4$) for dogfish, whereas urea permeability averaged $5.9 \pm 0.5 \times 10^{-7}$ cm/s for flounder and $4.3 \pm 1.7 \times 10^{-7}$ cm/s for dogfish. Figure 3 shows ammonia and proton fluxes in the

Table 1. Specific marker enzyme activities in different membrane fractions

	Flounder Gill		Shark Gill	
	ADPase	Na-K-ATPase	ADPase	Na-K-ATPase
Homogenate	2.5 \pm 0.2	3.0 \pm 0.3	5.3 \pm 1.6	1.15 \pm 0.2
Apical membranes	15.6 \pm 0.9	2.9 \pm 0.2	35.6 \pm 1.4	1.08 \pm 0.3
Enrichment	6.2 \times	0.97 \times	6.7 \times	0.9 \times
Basolateral membranes	NA	NA	3.2 \pm 1.4	2.6 \pm 0.3
Enrichment			0.6 \times	2.3 \times

Values are means \pm SE. Marker enzyme activities are expressed as $\mu\text{mol} \cdot \text{min}^{-1} \cdot \text{mg protein}^{-1}$. NA, not applicable.

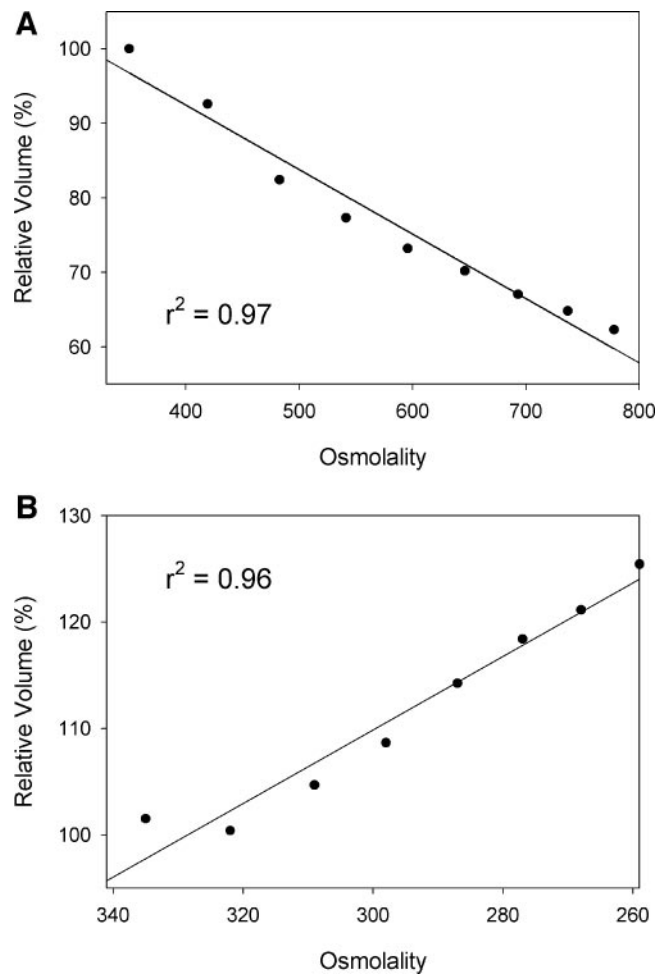


Fig. 1. Shark gill apical membrane vesicles exhibit linear volume changes in response to osmotic challenge. A: shrinkage; B: swelling. Washed membrane vesicles containing 2 mM carboxyfluorescein (CF) were exposed to increasing or decreasing osmolality after the addition of CF-quenching antibody and fluorescence was measured. Volume changes were calculated based on initial fluorescence and normalized to 100%. Linear regression coefficient (r) is shown. Data shown are representative of two experiments performed on separate preparations.

same preparations. In these assays, carboxyfluorescein is reporting on the intravesicular pH on exposure to either a proton gradient (Fig. 3, C and D) or to an NH_3 gradient (Fig. 3, A and B). In proton flux measurements, protons enter the vesicle from the more acidic outside solution, causing entrapped CF to quench. In NH_3 flux measurements, NH_3 enters the vesicle and is protonated to NH_4^+ , causing an intravesicular rise in pH and subsequent increase in fluorescence. Ammonia permeabilities averaged $1.9 \pm 0.3 \times 10^{-2}$ cm/s for flounder (Fig. 4A) and $1.4 \pm 0.1 \times 10^{-2}$ cm/s for dogfish (Fig. 4B), whereas proton permeabilities averaged 0.17 ± 0.04 cm/s in flounder (Fig. 4C) and 0.33 ± 0.07 cm/s in dogfish (Fig. 4D).

Because flux of water through aquaporins has a low activation energy (33), we measured and calculated the activation energies for water flux across each preparation. The activation energies for flounder and shark apical membranes and shark gill basolateral membranes were 12.0, 9.2, and 14.2 kcal/mol respectively, well above the values of 2–4 kcal/mol reported for water channel containing membranes.

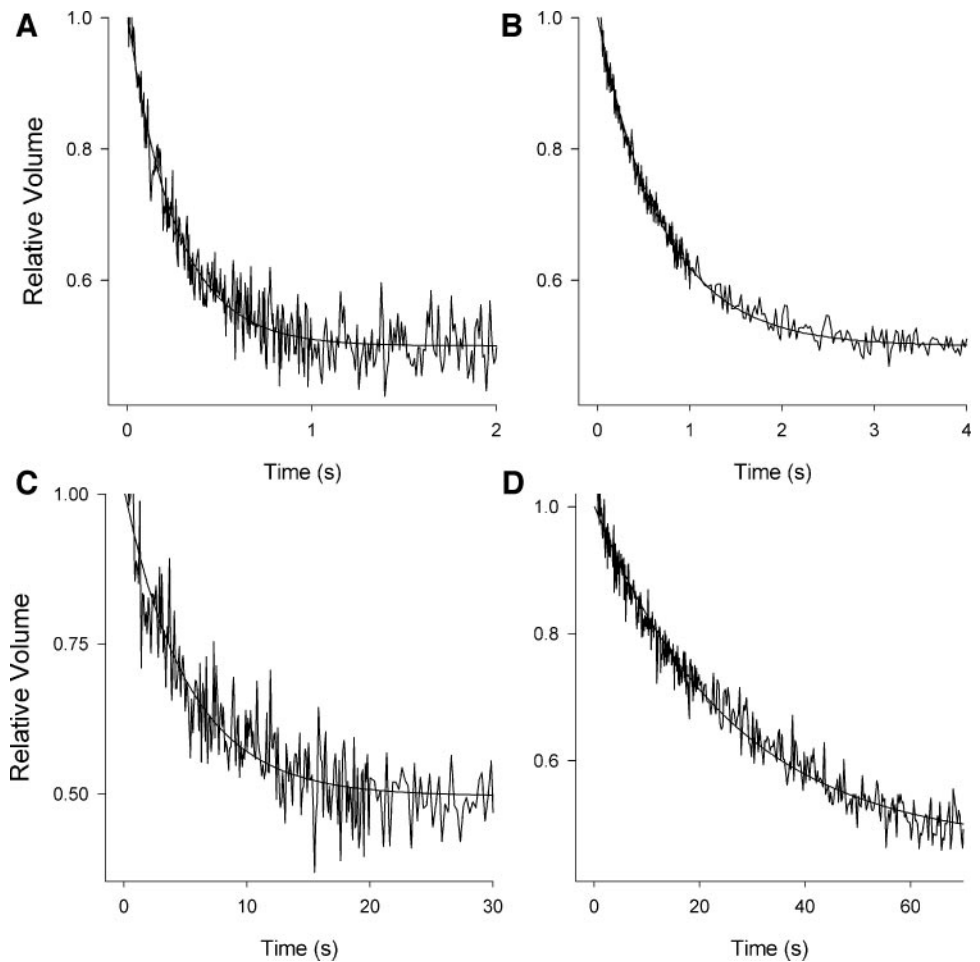


Fig. 2. Stopped-flow tracings showing water (A and B) and urea (C and D) efflux kinetics in flounder (A and C) and shark (B and D) gill apical membranes. Average stopped-flow traces (8–10) are shown from a single experiment. Fluorescence was converted to relative volume and a single exponential function was fitted to each curve.

It has been proposed that the dogfish gill restricts urea loss to the ocean by reducing the concentration of urea in the cytoplasm of the gill epithelial cells (9). To determine whether the basolateral membrane might provide an additional barrier to water and urea flux, we prepared gill basolateral membranes from dogfish. The method to isolate the apical membrane fraction is based on the difference in surface charge of the membranes. In the presence of calcium, their aggregation behavior is different. The method to isolate basolateral membranes takes advantage of the different size and/or shape of the membrane fragments, which leads to a different sedimentation rate during differential centrifugation in sucrose media.

Table 1 shows the relative purification of marker enzymes from gill basolateral membrane vesicles. We have reduced apical membrane and mitochondrial membrane markers (ADPase drops from 5.3 to $3.2 \mu\text{mol}\cdot\text{min}^{-1}\cdot\text{mg}^{-1}$ and succinate dehydrogenase from 5.7 to $3.1 \mu\text{mol}\cdot\text{min}^{-1}\cdot\text{mg}^{-1}$) to values approximately one-half that found in the homogenate and enriched the basolateral membrane by 2.3-fold. The enrichment factor appears to be low but because the basolateral membrane area is a much higher percentage per cell, and thus, per milligram of homogenate, it is in the range found for tissues with extensive basal and lateral infoldings such as the shark rectal gland (14). Figure 4, A–C, shows water, urea, and ammonia fluxes, respectively, across gill basolateral membrane vesicles. As shown in Table 2, at 15°C , water permeability averaged $1.4 \pm 0.2 \times 10^{-3} \text{ cm/s}$, urea permeability averaged

$6.5 \pm 1.1 \times 10^{-7} \text{ cm/s}$, and ammonia permeability averaged $0.013 \pm 0.003 \text{ cm/s}$ (all values are means \pm SE; $n = 3\text{--}4$ membrane preparations).

DISCUSSION

Teleosts and elasmobranchs maintain body fluid compositions strikingly different from those of the surrounding ocean despite the enormous surface area and high gas exchange rates of the gills (2, 3, 7, 16, 20). Teleosts must limit the flux of water across the gills and into the ocean (16). Elasmobranchs face a small osmotic gradient, which favors modest influx of water from the ocean into the fish, and an enormous urea gradient from fish to ocean (2, 3). Both teleosts and elasmobranchs likely excrete protons and ammonia across the gills as well (31). Because of these large apparent gradients, we hypothesized that gill apical membranes would exhibit extremely low permeabilities to water, urea, and ammonia. Because our previous studies on other barrier membranes revealed permeabilities in vitro that could account for barrier function in vivo, we expected to find exceptionally low permeabilities, which would then trigger a study of lipid structure to determine how gill lipid structure resulted in extremely low permeabilities.

We therefore isolated these membranes and measured their permeabilities. Membranes spontaneously vesiculated on homogenization and entrapped the volume and pH-reporter dye carboxyfluorescein. We concluded the vesicles formed were

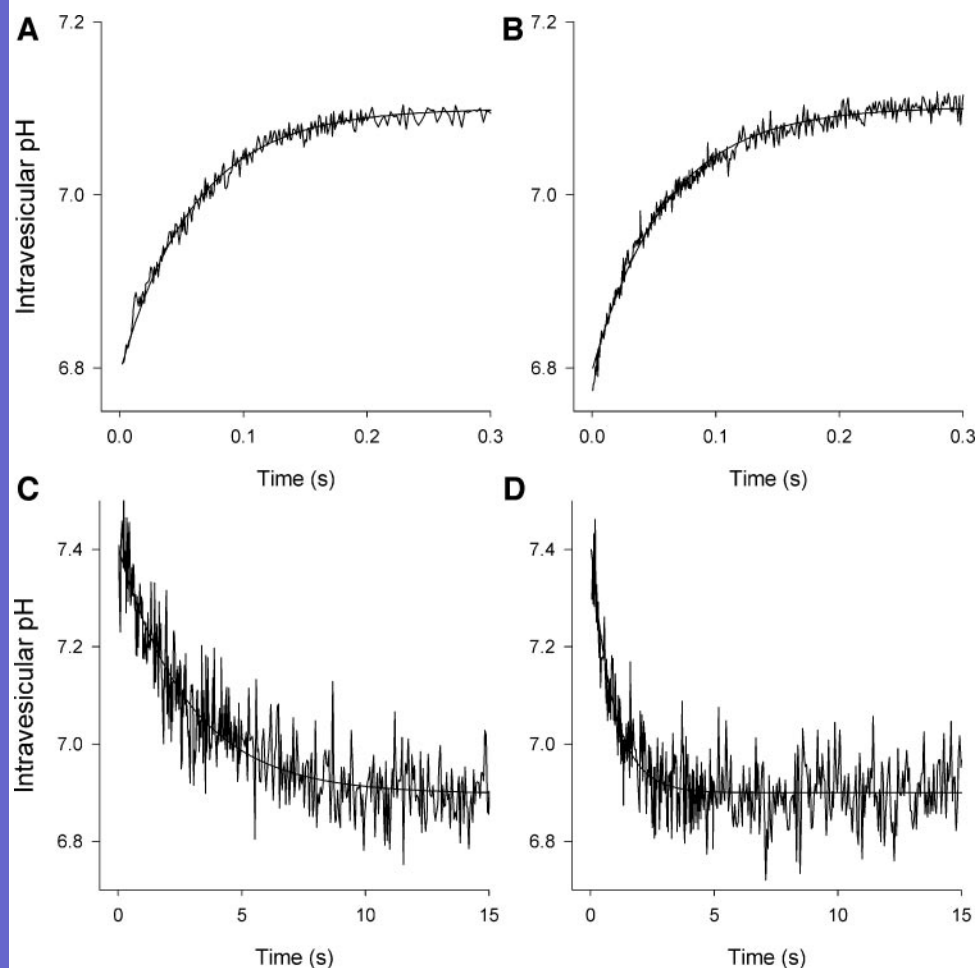


Fig. 3. Stopped-flow tracings showing NH_3 (A and B) and proton (C and D) flux kinetics in flounder (A and C) and shark (B and D) gill apical membrane vesicles. Average stopped-flow traces (8–10) are shown from a single experiment. Fluorescence was converted to intravesicular pH and a single exponential function was fitted to each curve.

not leaky under these experimental conditions because of the very different temporal kinetics displayed by different permeating solutes. These ranged from 300 ms (for NH_3) to 30 s (for urea). The measured values for apical membrane water and urea permeability compare favorably with those of other barrier apical membranes, including those of the mammalian bladder (22), medullary thick ascending limb of Henle (27), toad urinary bladder (13), Madin-Darby canine kidney cells (19), and gastric mucosa (26). All of these apical membranes exhibit water permeabilities in the range of $2\text{--}6 \times 10^{-4}$ cm/s at 25°C . The purification data indicate that a high proportion of the vesicles in each preparation represent apical membranes. In particular, the fact that each preparation behaved as a single population indicates that the permeabilities measured represent those of the apical membranes of gill epithelia.

To ensure that the gill apical membrane in fact represents the membrane most likely to function as a barrier, we examined as well the permeabilities of basolateral membranes prepared from dogfish gill epithelia. Permeability coefficients in the basolateral membrane preparations were 1.5- to 2-fold higher for water and urea than the apical membrane preparations. These higher values are amplified *in vivo* by the larger surface area of basolateral compared with apical membrane (18, 32) so that for urea and water it appears that diffusional fluxes across the basolateral membrane are 5–10 times higher than across the apical membrane. This estimate is based on the conservative

assumption of basolateral:apical surface area in columnar and squamous epithelia with extensive basolateral infoldings being anywhere from 3:1–6:1. These results are consistent with recent studies performed in intact dogfish gill perfusion experiments, in which urea was loaded into the epithelial cells and its washout into the bathing or perfusing medium was measured (23). The results showed that urea moved 14 times faster across the basolateral membrane into the perfusate than it moved across the apical membrane into the bathing medium (23). On this basis, the apical membrane appears to be the major barrier for the flux of most small solutes in the absence of specific transporters, and we can use the apical membrane permeability values to estimate the amount of flux that may occur in teleosts and elasmobranchs *in vivo*.

Comparison of measured permeabilities of vesicle preparations with values obtained in intact gill tissues. Although the permeabilities we have measured place gill apical membranes into the range of other barrier apical membranes, are these permeabilities low enough to account for the barrier function of the gill *in vivo*? The relationship between water flux rate (in mol/s) and osmotic permeability (P_f) is described by

$$\text{Flux} = P_f \times (\Delta\text{Osm}) \times (\text{MVW}) \times (\text{SA}) \quad (1)$$

where ΔOsm is the osmotic gradient (in mosmol/cm³), MVW is the molar volume of water (in 0.018 cm³/mmol), and SA is the surface area of the gill (in cm²/kg). In flounder, SA is 2,000

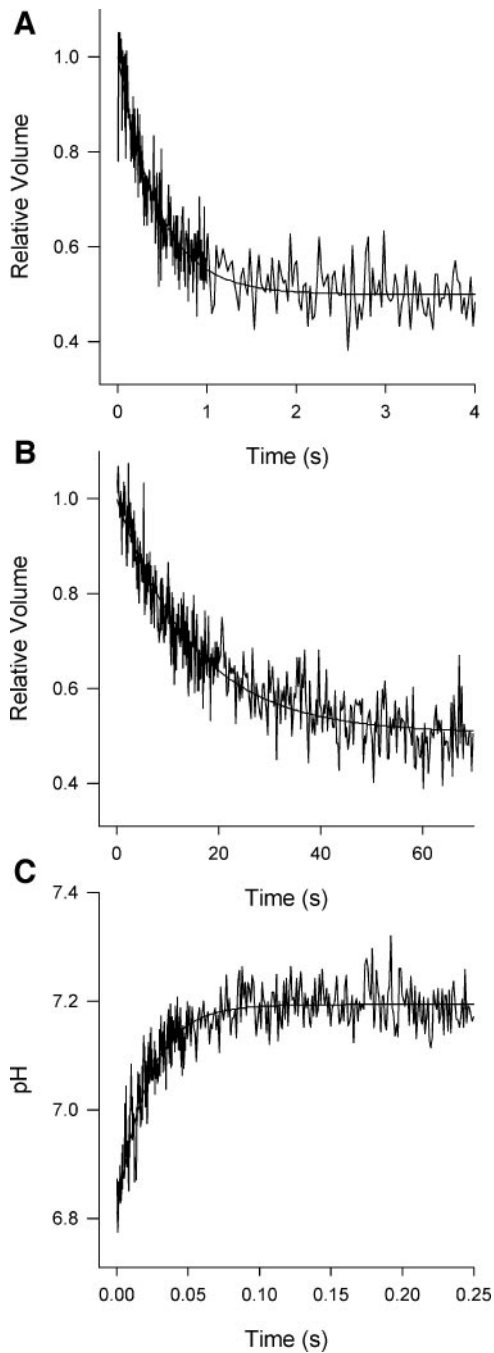


Fig. 4. Stopped-flow tracings showing water (A), urea (B), and NH_3 (C) flux kinetics in shark gill basolateral membrane vesicles. Average stopped-flow traces (8–10) are shown from a single experiment. Fluorescence was converted to relative volume or intravesicular pH and a single exponential function was fitted to each curve.

cm^2/kg (21). In dogfish, values of 3,000–3,700 cm^2/kg have been measured (2).

With the use of Eq. 1, permeability values obtained from apical membrane vesicles predict that a 300-g flounder would lose 370 ml/day in free water across the gills, whereas a 1-kg dogfish would absorb 193 ml/day of free water. These values appear to be quite high because the total body water of a 300-g flounder is ~ 210 ml (21). In dogfish, gill fluid absorption must be less than or equal to the sum of daily excretion of 40 ml/day from rectal gland and kidney combined (3). It therefore seems highly unlikely that the dogfish absorbs ~ 200 ml of water per day across its gills.

Consistent with these calculations, prior measurements of gill water permeability in vivo and in intact ex vivo preparations have yielded apparent permeability values far lower than ours (see Table 2). Measurements in rainbow trout conditioned to fresh water averaged 1.56×10^{-5} cm/s, whereas those for freshwater-adapted eel (30) averaged 1.46×10^{-5} cm/s. Measurements of dogfish gill place the apparent water permeability at $6.6 - 7.6 \times 10^{-6}$ cm/s, values about one-half of those observed in the teleost preparations (2, 9, 23). These values are ~ 100 times lower than the values we obtained in freshly isolated vesicle preparations.

With respect to urea or other solutes, the relationship between flux (in mol/s) and the permeability coefficient is expressed as

$$\text{Flux} = P_{\text{urea}} \times (\Delta \text{urea concentration}) \times (\text{SA}) \quad (2)$$

where P_{urea} is the urea permeability coefficient (in cm/s) and $\Delta \text{urea concentration}$ is the concentration gradient for urea (expressed in mol/cm³).

By using Eq. 2, anticipated urea loss across the dogfish gill is 41 mM per day in a 1-kg animal. Assuming a urea concentration in the animal of 330 mM/l (3), and a total body water of 70% of weight (21) plus equilibration of urea in all compartments, this rate of daily loss of urea represents $\sim 18\%$ of the animal's urea complement lost per day. Again, this value seems quite high (12), although not as dramatic as the water gain noted above.

Measurements of urea permeability in intact gill preparations reveal values of $2.2 - 2.6 \times 10^{-6}$ cm/s in trout and eel and values of $3.2 - 7.5 \times 10^{-8}$ cm/s in the dogfish (2, 9, 23). The teleost values are 4-fold higher than the values we have obtained in flounder apical membrane vesicles, whereas the dogfish values are 10-fold lower.

By using Eq. 2, we can also calculate the amount of ammonia loss that we would expect to occur in dogfish. If the plasma ammonia concentration is 0.25 mM and the plasma pH is 7.8 (31), then the animal would lose ~ 36 mM/day of ammonia. Clearly, this value is also high.

Table 2. Permeability coefficients

	Whole Gill Dogfish*	AM Vesicles Dogfish	BLM Vesicles Dogfish	Whole Gill Teleost†	AM Flounder
Water	$6.6 - 7.6 \times 10^{-6}$	$7.4 \pm 0.7 \times 10^{-4}$	$14 \pm 2 \times 10^{-4}$	$1.5 - 1.6 \times 10^{-5}$	$6.6 \pm 1.8 \times 10^{-4}$
Urea	$3.2 - 7.5 \times 10^{-8}$	$4.3 \pm 1.7 \times 10^{-7}$	$6.5 \pm 1.1 \times 10^{-7}$	$2.2 - 2.6 \times 10^{-6}$	$5.9 \pm 0.5 \times 10^{-7}$
Ammonia		$1.4 \pm 0.1 \times 10^{-2}$	$1.3 \pm 0.3 \times 10^{-2}$		$1.9 \pm 0.3 \times 10^{-2}$

Values are means \pm SE and represent permeability coefficients (in cm/s). AM, apical membrane; BLM, basolateral membranes. *Data for whole gill dogfish are from Refs. 2, 9, and 23. †Data for whole gill teleost are from Ref. 30; whole gill teleost was harvested from rainbow trout and eel.

There are several potential causes for the apparent discrepancies between vesicle measurements and both measured values and expected values in intact tissues. First, there are significant methodological differences between studies of perfused gill preparations and of isolated vesicles. Perfused preparations and the animal in vivo may have significant ventilation-perfusion mismatches, which will lead to marked diminutions in fluxes in intact tissues. Indeed, it is well known that the gill regulates gas exchange by varying the matching of blood perfusion with water flow over the exposed gill surface (11). By contrast, the entire membrane area of vesicle preparations is available for flux, leading to higher apparent transport values.

Second, the intact gill presents several potential areas for unstirred layer effects. One of these is the mucous layer which is especially abundant in seawater adapted fishes. Estimates from gas diffusion studies indicate that this layer is 1–3 μm thick in seawater-adapted gills (11). Depending on the composition and overall negative charge of the mucin, it may present a significant barrier to diffusion. Such a barrier could be more restrictive for some substances than for others. Because our apical membrane preparations exhibit dark staining indicative of an abundance of membrane glycoprotein, we repeated our permeability measurements in a seawater-like buffer, which duplicated the ionic strength and divalent cation composition of the ocean in Frenchman's Bay (3). This change in buffer composition had no effect on water permeability in dogfish gill apical membrane vesicles. Because mucin is reported to be less abundant in gills adapted to fresh water than in those adapted to seawater (11), it would be useful to compare the permeability properties of gill apical membrane vesicles isolated from a fish species adapted to fresh water compared with seawater. Multiple vesicle studies performed in our laboratories have confirmed that membrane vesicles exhibit no measurable unstirred layer effects for fluxes of water, urea, or ammonia. In addition, we have never encountered any situation where resealing of vesicles altered their permeability values (13, 26).

A third possibility relates to regulation of intracellular concentrations of molecules that readily cross the membrane. If the cell has an osmolality different from that of the plasma, or a lower concentration of urea or ammonia, fluxes of water, urea, and ammonia across the apical membrane may be reduced. Such a mechanism applies to CO_2 , which rapidly crosses cell membranes. The efflux of this gas is governed by its levels in the cytosol, and by dysequilibrium effects in the mucin layer lining the apical membrane, i.e., in the absence of carbonic anhydrase, there may be reasonable amounts of external CO_2 , which would diminish the size of the concentration gradient (6).

Which of these mechanisms likely play a significant role in barrier function for water, urea and ammonia? For water, it appears most likely that the cellular osmolality in well perfused epithelial areas of flounder and shark is similar to that of the plasma, because, at least for dogfish, the basolateral membrane is relatively permeable and has a large surface area. However, if gill areas are less well perfused, the osmolality of the cells may approach that of the seawater, reducing water flux. In addition, the mucin layer lining the apical surface may present a significant diffusion barrier. Because the mucin layer is composed of both integral membrane mucins and secreted mucins, it is very difficult to duplicate it in vitro.

For urea, the mechanisms described for water may apply, but there may also be reduced levels of urea within the gill

epithelial cell, due to a backflux transporter mechanism (9). Such a mechanism would involve some sort of secondary active transport pathway which would maintain the cytoplasmic urea level below that of plasma. The fact that our water measurements differ from the intact tissue by a factor of 100, whereas our urea fluxes in dogfish differ by a factor of 10, may be due to a highly selective unstirred layer in the mucin lining the apical membrane of the epithelial cells.

It is clear that ammonia leakage into the ocean, like that of another more highly permeable gas, CO_2 , is governed not by the membrane permeability but by chemical gradients between the cytoplasm and the mucin layer lining the apical membrane (6, 11). Carbonic anhydrase in this layer catalyses the rapid hydration of CO_2 to bicarbonate and a proton. The resulting protons can combine with excreted NH_3 to form NH_4^+ , thus rapidly reducing the levels of NH_3 in the mucous layer and augmenting excretion. If levels of ammonia are kept low in the cytosol, then the rate of ammonia efflux would be governed by cytosolic ammonia levels and the pH of the apical mucous layer.

In conclusion, we have measured the water, urea, and ammonia permeabilities of apical membranes from the gill epithelia of a teleost and an elasmobranch as well as those of the basolateral membrane of the elasmobranch. The apical membrane clearly serves as the best barrier membrane in the epithelium. Although the apical membrane permeabilities we have measured place the gill apical membranes well into the range of other barrier apical membranes that have been studied, the permeabilities are not low enough to account for gill barrier function in vivo. It appears highly likely that ventilation/perfusion mismatches, diffusion barriers such as the mucin layer, and regulation of chemical gradients across the apical membrane play a prominent role, along with the barrier apical membrane in determining the efficacy of the gill permeability barrier. The fact that so many barrier membranes exhibit similar permeabilities suggests that there is a biological limit to how low the permeability of a barrier membrane can go and yet remain in the fluid state in vivo.

ACKNOWLEDGMENTS

We thank Wily G. Ruiz for technical assistance with electron microscopy and Drs. David Evans, Frank Epstein, and John Forrest for helpful discussions.

GRANTS

This work was supported by National Institutes of Health Grants DK-43955 (to M. L. Zeidel) and DK-51970 (to G. Apodaca) and a new investigator award from Mount Desert Island Biological Laboratory (to M. L. Zeidel).

REFERENCES

- Booth AG and Kenny AJ. A rapid method for the preparation of microvilli from rabbit kidney. *Biochem J* 142: 575–581, 1974.
- Boylan JW. Gill permeability in *Squalus acanthias*. In: *Sharks, Skates and Rays*, edited by Gilbert PW, Mathewson RF, and Rall DP. Baltimore, MD: Johns Hopkins Press, 1967.
- Burger JW. Problems in the electrolyte economy of the spiny dogfish, *Squalus acanthias*. In: *Sharks, Skates and Rays*, edited by Gilbert PW, Mathewson RF, and Rall DP. Baltimore, MD: Johns Hopkins Press, 1967.
- Carrier JC and Evans DH. Ion, water and urea turnover rates in the nurse shark, *Ginglymostoma cirratum*. *Comp Biochem Physiol A* 41: 761–764, 1972.
- Chang A, Hammond TG, Sun TT, and Zeidel ML. Permeability properties of the mammalian bladder apical membrane. *Am J Physiol Cell Physiol* 267: C1483–C1492, 1994.





6. **Claiborne JB, Edwards SL, and Morrison-Shetlar AI.** Acid-base regulation in fishes: cellular and molecular mechanisms. *J Exp Zool* 293: 302–319, 2002.
7. **Cutler CP and Cramb G.** Molecular physiology of osmoregulation in eels and other teleosts: the role of transporter isoforms and gene duplication. *Comp Biochem Physiol A* 130: 551–564, 2001.
8. **Deamer DW and Nichols JW.** Proton-hydroxide permeability of liposomes. *Proc Natl Acad Sci USA* 80: 165–168, 1983.
9. **Fines GA, Ballantyne JS, and Wright PA.** Active urea transport and an unusual basolateral membrane composition in the gills of a marine elasmobranch. *Am J Physiol Regul Integr Comp Physiol* 280: R16–R24, 2001.
10. **Fiske CH and Subbarow Y.** The colorimetric determination of phosphorous. *J Biol Chem* 66: 375–388, 1925.
11. **Gilmour Gas exchange KM.** In: *The Physiology of Fishes*, edited by Evans DH. New York: CRC, 1997.
12. **Goldstein L.** Urea biosynthesis in elasmobranchs. In: *Sharks, Skates and Rays*, edited by Gilbert PW, Mathewson RF, and Rall DP. Baltimore, MD: Johns Hopkins Press, 1967.
13. **Grossman EB, Harris HW Jr, Star RA, and Zeidel ML.** Water and nonelectrolyte permeabilities of apical membranes of toad urinary bladder granular cells. *Am J Physiol Cell Physiol* 262: C1109–C1118, 1992.
14. **Hannafin J, Kinne-Saffran E, Friedman D, and Kinne R.** Presence of a sodium-potassium chloride cotransport system in the rectal gland of *Squalus acanthias*. *J Membr Biol* 75: 73–83, 1983.
15. **Hill WG and Zeidel ML.** Reconstituting the barrier properties of a water-tight epithelial membrane by design of leaflet-specific liposomes. *J Biol Chem* 275: 30176–30185, 2000.
16. **Karnaky KJ.** Osmotic and ionic regulation. In: *The Physiology of Fishes* (2nd ed.), edited by Evans DH. New York: CRC, 1997.
17. **Lande MB, Priver NA, and Zeidel ML.** Determinants of apical membrane permeabilities of barrier epithelia. *Am J Physiol Cell Physiol* 267: C367–C374, 1994.
18. **Laurent P and Dunel S.** Morphology of gill epithelia in fish. *Am J Physiol Regul Integr Comp Physiol* 238: R147–R159, 1980.
19. **Lavelle JP, Negrete HO, Poland PA, Kinlough CL, Meyers SD, Hughey RP, and Zeidel ML.** Low permeabilities of MDCK cell monolayers: a model barrier epithelium. *Am J Physiol Renal Physiol* 273: F67–F75, 1997.
20. **Maetz J.** Aspects of adaptation to hypo-osmotic and hyper-osmotic environments. In: *Biochemical and Biophysical Perspectives in Marine Biology*, edited by Malins DC and Sargent JR. London: Academic, vol. 1, 1974.
21. **Motais R, Isaia J, Rankin JC, and Maetz J.** Adaptive changes of the water permeability of the teleostean gill epithelium in relation to external salinity. *J Exp Biol* 51: 529–546, 1969.
22. **Negrete HO, Lavelle JP, Berg J, Lewis SA, and Zeidel ML.** Permeability properties of the intact mammalian bladder epithelium. *Am J Physiol Renal Fluid Electrolyte Physiol* 271: F886–F894, 1996.
23. **Part P, Wright PA, and Wood CM.** Urea and water permeability in dogfish (*Squalus acanthias*) gills. *Comp Biochem Physiol A* 119: 117–123, 1998.
24. **Payan P and Maetz J.** Balance hydrique chez les Elasmobranches: arguments en faveur d'un controle endocrinien. *Gen Comp Endocrinol* 16: 535–544, 1971.
25. **Powell MD, Speare DJ, and Wright GM.** Comparative ultrastructural morphology of lamellar, epithelial, chloride and mucous cell glycocalyx of the rainbow trout (*Oncorhynchus mykiss*) gill. *J Fish Biol* 44: 725–730, 1994.
26. **Priver NA, Rabon EC, and Zeidel ML.** Apical membrane of the gastric parietal cell: water, proton, and nonelectrolyte permeabilities. *Biochemistry* 32: 2459–2468, 1993.
27. **Rivers R, Blanchard A, Eladari D, Levief F, Paillard M, Podevin RA, and Zeidel ML.** Water and solute permeabilities of medullary thick ascending limb apical and basolateral membranes. *Am J Physiol Renal Physiol* 274: F453–F462, 1998.
28. **Robin ED and Murdaugh HV.** Gill gas exchange in the elasmobranch *Squalus acanthias*. In: *Sharks, Skates and Rays*, edited by Gilbert PW, Mathewson RF, and Rall DP. Baltimore, MD: Johns Hopkins Press, 1967.
29. **Saenz J, Kinne RKH, and Kinne-Saffran E.** Determination of the purity of membrane fractions isolated from flounder (*Pleuronectes americanus*) gills by a selective biotin exposure technique. *Mount Desert Island Biol Lab Bull* 42: 85–88, 2003.
30. **Steen JB and Stray-Pedersen S.** The permeability of fish gills with comments on the osmotic behavior of cellular membranes. *Acta Physiol Scand* 95: 6–20, 1975.
31. **Wilkie MP.** Ammonia excretion and urea handling by fish gills: understanding and future research challenges. *J Exp Zool* 293: 284–301, 2002.
32. **Wright DE.** The structure of gills of the elasmobranch, *Scyliorhinus canicula*. *Z Zelforsch Mikrosk Anat* 144: 489–509, 1973.
33. **Zeidel ML, Ambudkar SV, Smith BL, and Agre P.** Reconstitution of functional water channels in liposomes containing purified red cell CHIP28 protein. *Biochemistry* 31: 7436–7440, 1992.